Supplemental Materials

Quantum-Enhanced Tunable Second-Order Optical Nonlinearity in Bilayer Graphene

Sanfeng Wu[1], Li Mao[2], Aaron M. Jones[1], Wang Yao[3], Chuanwei Zhang[2], Xiaodong Xu[1,4*]

[1] Department of Physics, University of Washington, Seattle, Washington 98195, USA
[2] Department of Physics and Astronomy, Washington State University, Pullman, Washington 99164 USA
[3] Department of Physics and Center of Theoretical and Computational Physics, The University of Hong Kong, Hong Kong, China
[4] Department of Material Science and Engineering, University of Washington, Seattle, Washington 98195, USA
*Email: xuxd@uw.edu

1. Theory for second order optical conductivity

Considering the applied potential bias between top and bottom gates, the electronic Hamiltonian near the Dirac points (***K*** and ***K'***) is[1]:

$$H = \sum \psi_{\boldsymbol{k}}^{\dagger} \mathcal{H}_{\boldsymbol{k}} \psi_{\boldsymbol{k}},$$

where

$$\psi_{\boldsymbol{k}}^{\dagger} = (b_{\boldsymbol{k}}^{1\dagger}, a_{\boldsymbol{k}}^{1\dagger}, a_{\boldsymbol{k}}^{2\dagger}, b_{\boldsymbol{k}}^{2\dagger}),$$

and

$$\mathcal{H}_{\boldsymbol{k}} = \begin{pmatrix} -\Delta & \hbar v_f g & 0 & 0 \\ \hbar v_f g^* & -\Delta & \gamma_1 & 0 \\ 0 & \gamma_1 & \Delta & \hbar v_f g \\ 0 & 0 & \hbar v_f g^* & \Delta \end{pmatrix},$$

$a_k^{i\dagger}(b_k^{i\dagger})$ is the creation operator for electrons at the sublattice A (B), in the layer $i(\mathrm{i} = 1,2)$, and with momentum k in the BZ. $\mathrm{k} = (\mathrm{k_x}, \mathrm{k_y})$ is the continuous wave vector from K, K' and $\mathrm{g} = \mathrm{k_x} - \xi\,\mathrm{i}\,\mathrm{k_y}$ is a complex number ($\xi = +1$ for K and $\xi = -1$ for K'). The Fermi velocity v_f is determined by the intra-layer hopping energy $\gamma_0 \approx 2.8\,eV$ between nearest neighbors. a is the lattice constant of graphene. $\gamma_1 \approx 0.4\,eV$ is the inter-layer hopping parameter between A_1 and A_2. We ignore other hopping processes due to their relatively weak strengths. The diagonal items $\pm\Delta$ come from the potential bias between the two graphene-layers. Diagonalizing the Hamiltonian, we can obtain the energy spectrum with four branches near the Dirac point[1].

The interaction between light and BLG can be described by replacing the momentum vector $\hbar\boldsymbol{k}$ with[1]

$$\boldsymbol{p} = \hbar\boldsymbol{k} + e\boldsymbol{A},$$

where $\boldsymbol{A} = -\boldsymbol{E}/(\boldsymbol{i}\omega)$ is the vector potential of the incident laser beam. As an example, if the incident laser is a circularly polarized beam σ_+, then $\mathrm{E} = \frac{\mathrm{E}e^{\mathrm{i}\omega t}}{2\mathrm{i}}(1, -\mathrm{i}) + \mathrm{c.c.}$ The interaction between laser and electrons (~1meV) is weak compared to the system energy scale (~0.1eV), therefore we can write the total Hamiltonian under band representation as

$$\bar{\mathcal{H}}_{\boldsymbol{p}} = \bar{\mathcal{H}}_{\boldsymbol{k}} + \frac{ev_f E e^{i\omega t}}{2\omega} \mathrm{H}_\Phi.$$

where $\mathrm{H}_\Phi = \Phi^\dagger[\boldsymbol{I}\otimes(\sigma_x - i\xi\sigma_y)]\Phi$ for a circularly polarized beam $\boldsymbol{\sigma}_+$. $\boldsymbol{I}$ is a 2 × 2 unit matrix. $\boldsymbol{\sigma} = (\sigma_x, \sigma_y)$ is the vector of Pauli matrixes. Φ is the initial eigenstate without the laser-field satisfying $\bar{\mathcal{H}}_k = \Phi^\dagger \mathcal{H}_k \Phi = \mathrm{diag}[\epsilon_1, \epsilon_2, \epsilon_3, \epsilon_4]$, where $\epsilon_i (i = 1,2,3,4)$ is the energy of the i[th] band.

The evolution of electronic states is determined by the quantum Liouville equation[2,3]

$$i\hbar\partial_t \rho = \left[\bar{\mathcal{H}}_{\boldsymbol{p}}, \rho\right] - \boldsymbol{i}\Gamma(\rho - \rho(t=0)),$$

where ρ is the time dependent quantum state of electrons with momentum $\boldsymbol{k}$ at temperature T and chemical potential μ. Γ describes the electronic relaxation time[4,5]. The linear and nonlinear optical response of ρ to the optical fields can be obtained by solving the Liouville equation perturbatively

$$\rho = \rho_{\boldsymbol{k}} + \left[\rho_1(t)e^{i\omega t} + c.c\right]E + [\rho_2(t)e^{i2\omega t} + c.c]E^2 + \cdots.$$

The initial state $\rho_{\boldsymbol{k}} = \mathrm{diag}\,[f_1, f_2, f_3, f_4]$ is the initial state obtained from the Fermi-Dirac distribution $f_i = \frac{1}{\exp[(\epsilon_i - \mu)/k_B T]+1}$ of electrons .

As we mentioned in the main text, the SHG does not exist unless there is an in-plane electric field. According to semi-classical electron transport theory, if there is an in-plane electric field $\mathcal{E}$, the Fermi surface is shifted by wavenumber $\Delta\boldsymbol{k} = e\tau\mathcal{E}/\hbar = m^* v_d/\hbar$ along the direction opposite the electric field owing to the negative electron charge. τ is the relaxation time, m^* is the electronic effective mass and v_d is the drift velocity. This process is responsible for the leak current $j_{\mathrm{sc}} = \sigma_{\mathrm{dc}}\mathcal{E}\mathrm{d}$ measured by the ammeter, where d is the sample length perpendicular to the electric field, assuming a rectangular sample shape. Replacing v_d with the electronic mobility $u_m = |v_d/\mathcal{E}|$, we have

$$\hbar\Delta\boldsymbol{k} = \frac{m^* u_m j_{\mathrm{sc}}}{\sigma_{\mathrm{dc}}\mathrm{d}}.$$

According to experimental data of BLG[6,7], we choose $m^* \approx 0.05m_e, u_m \approx 1\frac{m^2}{Vs}, \sigma_{\mathrm{dc}} \approx \frac{e^2}{\hbar}, v_f \approx 10^6 m/$, then $\hbar v_f \Delta\boldsymbol{k} \approx 0.01eV$ for a leak current $j_{\mathrm{sc}} \approx 8\ \mu\mathrm{A}/\mu m$ (corresponding to $\mathcal{E} \approx 2000\mathrm{V/m}$).

As a result of the shift of the Fermi surface, the initial electronic state in the presence of the in-plane applied current turns out to be

$$\rho_{\boldsymbol{k}} \longleftarrow \rho_{\boldsymbol{k}-\Delta\boldsymbol{k}}.$$

Substituting this into the quantum Liouville equation, we obtain the first order and second order equations for the electronic-state evolution

$$i\hbar\partial_t\rho_1 - (\hbar\omega - i\Gamma)\rho_1 = [\bar{\mathcal{H}}_{\boldsymbol{k}}, \rho_1] + \frac{ev_f}{2\omega}[\mathrm{H}_\Phi, \rho_{\boldsymbol{k}}],$$

$$i\hbar\partial_t\rho_2 - (2\hbar\omega - i\Gamma)\rho_2 = [\bar{\mathcal{H}}_{\boldsymbol{k}}, \rho_2] + \frac{ev_f}{2\omega}[\mathrm{H}_\Phi, \rho_1].$$

The dynamics of the electronic state excited by photons can be obtained by solving these two linear ordinary differential equations as a steady state problem (*i.e.*, $\partial_t\rho_1 = 0, \partial_t\rho_2 = 0$), yielding

$${\rho_1}^{ij} = -\left(\frac{ev_f}{2\omega}\right)\frac{[\mathrm{H}_\Phi, \rho_{\boldsymbol{k}}]_{ij}}{\hbar\omega + \epsilon_{ij} - i\Gamma},$$

$$\rho_2{}^{ij} = -(\frac{ev_f}{2\omega})\frac{[\mathrm{H}_\Phi, \rho_1]_{ij}}{2\hbar\omega + \epsilon_{ij} - i\Gamma}.$$

The induced electric current is defined as

$$j_e = \nu e \sum_{BZ} \mathrm{tr}(\rho \frac{\partial \bar{\mathcal{H}}_{\boldsymbol{p}}}{\partial \boldsymbol{p}}) = \sigma_1 E e^{i\omega t} + \sigma_2 E^2 e^{i2\omega t} + c.c + \cdots.$$

where $\nu = 2$ describes the spin degeneracy and σ_1 is the linear optical conductivity. We have confirmed that our result for σ_1 is exactly the same as that in former literature on BLG using the Kubo formula. Here we focus on the second order nonlinear optical conductivity σ_2, which stimulates SHG. The result is

$$\sigma_2^\alpha = 2e\sum_{BZ} tr\left(\rho_2 \frac{\partial \bar{\mathcal{H}}_{\boldsymbol{p}}}{\partial p_\alpha}\right) = 2ev_f \sum_{K,K'} tr(\rho_2 \eta_\Phi^\alpha)$$

$$= \frac{e^3 v_f^2}{8\pi^2\omega^2}\int_{BZ}\sum_{ijl}\left[\frac{\rho_k{}^{ii} - \rho_k{}^{ll}}{\hbar\omega + \epsilon_i - \epsilon_l - i\,\Gamma} - \frac{\rho_k{}^{ll} - \rho_k{}^{jj}}{\hbar\omega + \epsilon_l - \epsilon_j - i\,\Gamma}\right]\frac{(H_\Phi)_{il}\,(H_\Phi)_{lj}(\eta_\Phi^\alpha)_{ji}}{2\hbar\omega + \epsilon_i - \epsilon_j - i\,\Gamma}\,d\boldsymbol{k}.$$

Here $\eta_\Phi^\alpha = \frac{\partial \mathcal{H}_{\boldsymbol{p}}}{\partial p_\alpha} = v_f \Phi^\dagger (I \otimes \sigma_\alpha)\,\Phi$ for Dirac cone K and $\eta_\Phi^\alpha = v_f \Phi^\dagger (I \otimes \sigma_\alpha^*)\,\Phi$ for K′. i, j, l = 1,2,3,4 and the integration over k is performed in the vicinity of K or K′. $\alpha = x, y$ represents the axis direction in the graphene plane.

2. Effects of Γ

We set $\Gamma = 0.05$eV in our calculation in the main text. The value of Γ affects the magnitude of the second order optical conductivity significantly. In Fig. 1S. we show σ_2 as a function of Γ and the incident laser frequency ω. The incident laser is polarized along the x direction and T=30K. Apparently, the signal intensity becomes larger when the relaxation time of the excited electronic state becomes longer, i.e., smaller Γ.

3. Effects of the direction of the in-plane DC current

To achieve SHG, we have to apply an in-plane electric field. In the main text, we apply an in-plane current along the y direction as an example. In general, the direction of the field is not unique. One can obtain giant optical nonlinear conductivity by inducing a current in any direction in the 2D atomic plane. This is important in practice because the in-plane current may not lie in the y direction defined by the atomic structure (See Fig.1 in the main text). Here we show the results for a different direction ($-y'$) of the in-plane current with a linearly polarized incident laser at T=30 K (See Fig. 2S). We show that it is the direction of the DC current that determines the symmetric axis for second order optical conductivity (Fig. 2S **c** and **d**).

4. Intrinsic processes at 0.4eV peak

Here we show that the double resonant enhanced peak at $\omega = 0.4$eV arises from two different transitions, i.e., 1-3 (transition from the 1st band to the 3rd band) and 2-4 (transition from the 2nd band to the 4th band). Figure 3S plots the contribution from both processes respectively at T=30K without band gap opening. We can see that both processes contribute to an enhanced second order optical nonlinearity and the ratio between the 1-3 and 2-4 processes is about 1:2. We note that the ratio is almost invariant

with temperature.

5. Intrinsic processes at 0.2eV peak

The resonance peak at $\omega = 0.2$eV also arises from two different transition processes, i.e., 3-4 process and 2-3 process. In the situation described in our scheme, the 2-3 process is the leading one (see Fig. 4S **a** and **b**). The resonance peak of the 2-3 process has a shift from 0.2eV as temperature increases (Fig. 4S **a**), arising from the interplay of temperature T, Fermi level shifting Δk and energy band broadening Γ. This effect leads to the shift of the resonant position of the 2-3 transition toward the Dirac point, which corresponds to an obvious shift of the peak in the spectrum. We plot the shift amount $\Delta\omega$ as a function of temperature when $\Delta k = 0.01eV$ and Γ=0.05eV in Fig. 4S **c**.

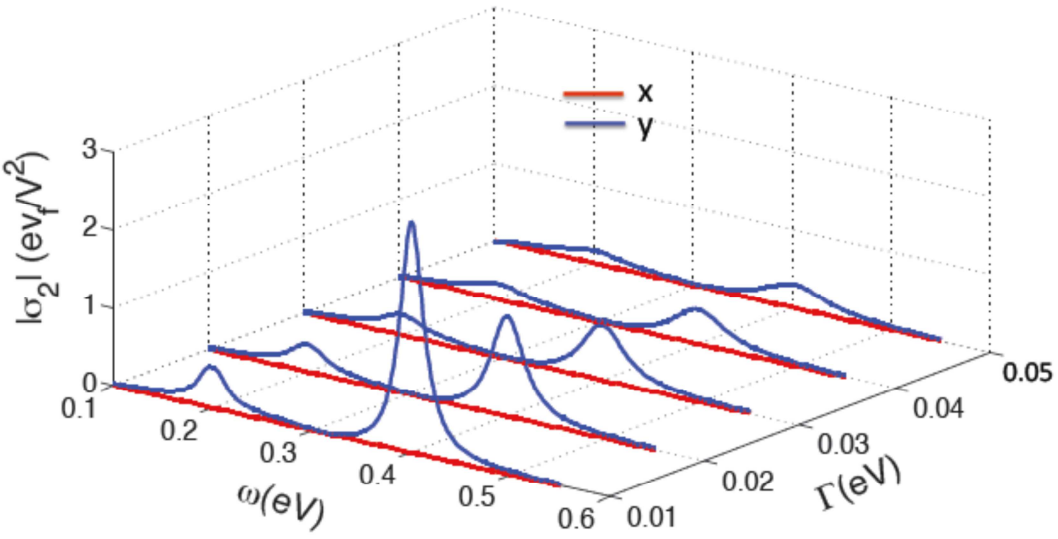

Figure 1S | Effects of relaxation time of excited states on SHG. The incident laser is linearly polarized and T=30 K. Blue line denotes the second order optical conductivity in the y direction and red in the x direction.

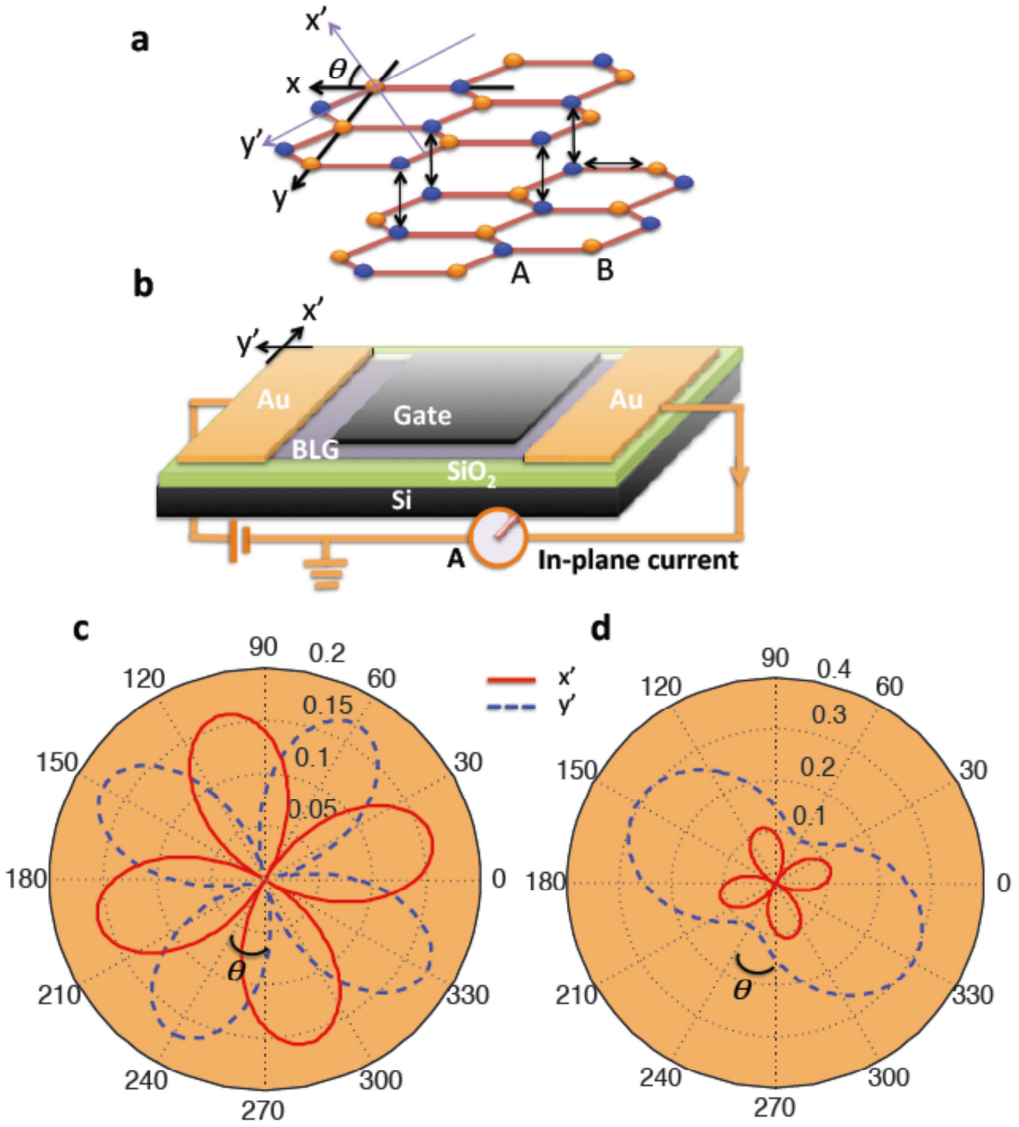

Figure 2S | Effect of the direction of in-plane electric field on SHG. **a**, Atomic structure of BLG. (x,y) and the coordinates used for tight-binding model. ($-y'$) is the direction of the DC current as shown in **b**. **b**, Normal device scheme of BLG, which determines the direction of the current, which is usually not along the axis of the coordinates (x,y) in **a**. The deviation is described by an angle θ. **c** and **d**, polar plots of the intensity of the second order optical conductivity in the x' and y' direction at T=30 K for incident laser frequency (**c**) $\omega = 0.2$ eV and (**d**) $\omega = 0.4$ eV. We can see that the direction of the in-plane field determines the symmetric axis (shown by θ) of the optical nonlinearity. Polar angle is the polarization angle of the incident beam starting from the x-axis.

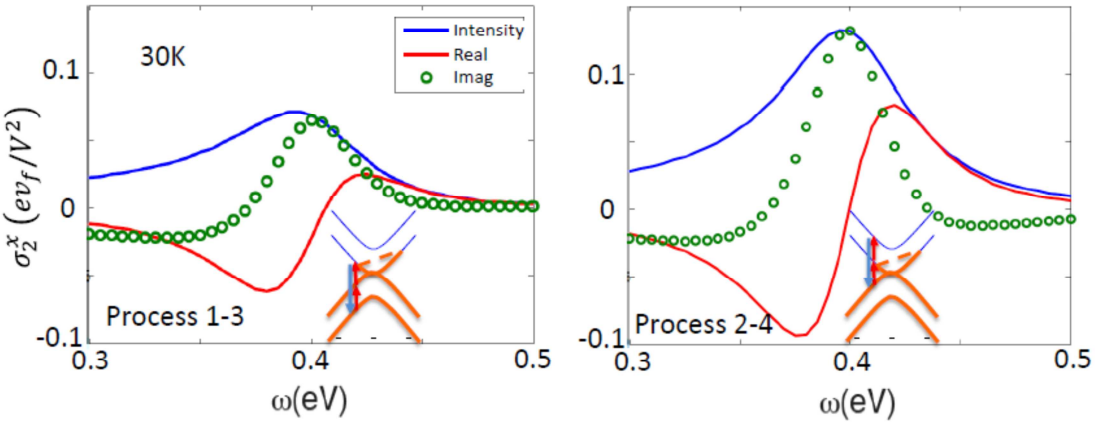

Figure 3S | Contributions to the second order optical nonlinearity at $\omega = 0.4$ eV from 1-3 and 2-4 transitions, respectively. Laser is left handed polarized and Temperature is set to be 30K.

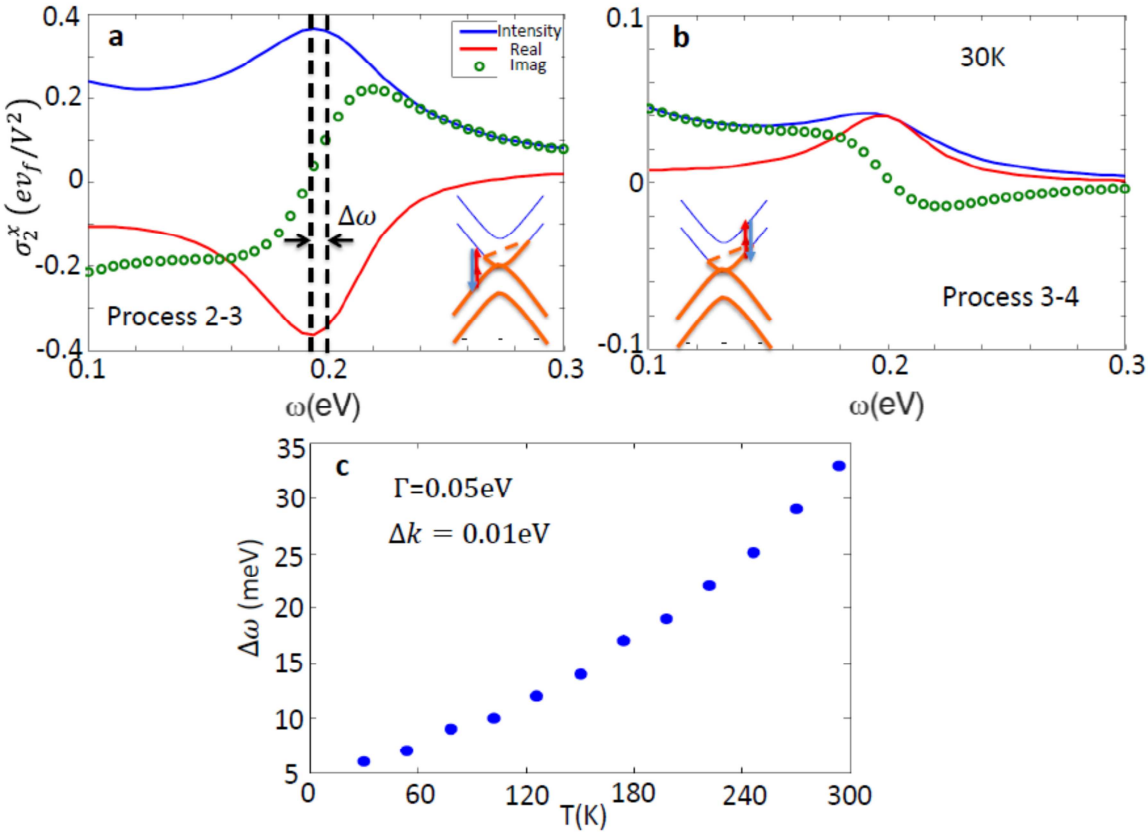

Figure 4S | Contributions to the second order optical nonlinearity at $\omega = 0.2$eV from 2-3 and 3-4 transitions, respectively (**a** and **b**). We can clearly see that the transition is dominated by the 2-3 process. The peak position has a shift $\Delta\omega$ under increasing temperature, plotted in **c.**

Reference:

(1) Neto, A. H. C., *et al*., The electronic properties of graphene, *Rev. Mod. Phys*. **81**, 109 (2009).

(2) Hendry, E., *et al*, Coherent Nonlinear Optical Response of Graphene, *Phys. Rev. Lett*. **105**, 097401 (2010)

(3) Landau, L. D., & Lifshitz, E. M. (1977). Quantum Mechanics, Non-Relativistic Theory: Volume 3. Oxford: Pergamon Press. pp. 41. ISBN 0080178014.; Sakurai, J.J., Modern Quantum Mechanics, revised edition, by Addison-Wesley Publishing Company, Inc. 1994

(4) Nandkishore, R., & Levitov, L., Polar Kerr Effect and Time Reversal Symmetry Breaking in Bilayer Graphene, *Phys. Rev. Lett*. **107**, 097402 (2011)

(5) Yang, H., Feng,X., Wang, Q., Huang, H., Wei Chen, W., Wee, A. T. S., & Ji, W., Giant Two-Photon Absorption in Bilayer Graphene, *Nano Lett*., **11** (7), pp 2622–2627, (2011).

(6) Zhang L. M., *et al*, Determination of the electronic structure of bilayer graphene from infrared spectroscopy, *Phys. Rev. B* **78**, 235408 (2008)

(7) Zou K., *et al*, Effective mass of electrons and holes in bilayer graphene: Electron-hole asymmetry and electron-electron interaction, Phys. Rev. B 84, 085408 (2011)